Applied Catalysis A: General 345 (2008) 164–175

Contents lists available at ScienceDirect

Applied Catalysis A: General

journal homepage: www.elsevier.com/locate/apcata

# Effect of pretreatment conditions on the catalytic performance of Ni-Pt-W supported on amorphous silica-alumina catalysts
## Part 2. Catalysts prepared by a hybrid method

Miloud Guemini, Yacine Rezgui *

*Laboratoire de Recherche de Chimie Appliquée et Technologie des Matériaux, Université d'Oum El Bouaghi, B.P. 358, Route de Constantine, Oum El Bouaghi 04000, Algeria*

ARTICLE INFO

*Article history:*
Received 17 January 2008
Received in revised form 24 April 2008
Accepted 27 April 2008
Available online 3 May 2008

*Keywords:*
Platinum
Tungsten-oxide
Nickel
Isomerization
Pretreatment conditions
Hybrid technique

ABSTRACT

Activation procedures of Ni-W-Pt based catalysts, prepared by means of a hybrid technique: sol–gel and incipient wetness impregnation, were investigated in terms of their activity in reaction of *n*-hexane isomerization in a continuous fixed-bed quartz reactor operating at atmospheric pressure, by changing operating conditions such as time on stream, $SiO_2/Al_2O_3$ and $H_2$/*n*-hexane ratios. This study aims to understand the effects of the pretreatment conditions, such as calcination and reduction temperature, over some properties of these catalysts and to analyze the relationship between the metal content, the acidity (strength) of the samples and their catalytic performance.

The chemical composition of the prepared solids have bas characterized by inductively coupled plasma-atomic emission spectroscopy (ICP-AES), their specific surface areas were measured using BET method, while their reduction behavior was characterized by temperature-programmed reduction and their acidity was assessed by means of ammonia temperature-programmed desorption. The collected data revealed that both BET surface areas and catalytic activity as well as surface acidity of these solids are strongly dependent on their pretreatment conditions. Besides, the reduction behavior of the prepared materials was related to nickel and platinum amounts, the higher the concentrations of these species the easier the reducibility of the samples. On the other hand, it was found that all ($Ni_xPt_y$) catalysts deactivate with time on stream, with the conversion remaining steady after 100 min. Moreover, the obtained results on $(Ni_{12}Pt_{0.4})_{AC}$ catalyst showed that the $SiO_2/Al_2O_3$ ratio and $H_2$ partial pressure affect isomerization selectivity positively while opposite effect was observed for activity (conversion). In addition, the main products in *n*-hexane hydroconversion were found to be monobranched isomers which dominate all practical conversions and their formation increases together with that of multibranched ones. Besides, the cracked products are not produced in significant amounts until about 30% conversion.



## 1. Introduction

The health hazards associated with lead emission and the use of catalytic converters in most cars have required the reformulation of gasolines [1]. Consequently, today most petroleum refineries are facing the challenge of producing motor gasoline having all the desirable properties and also comply with the ever-increasing environmental regulations on automotive emissions [2–4]. These regulations promote the utilization of clean gasolines with high RON and with low content of aromatics (benzene in particular) [5], of olefins and of sulfur compounds [6,7]. Hydrocarbons of gasoline boiling range can be produced by alkylation (a very costly technology) or by isomerization of *n*-paraffins [8,9].

Nowadays, the skeletal isomerization for normal paraffin to isoparaffin is regarded as one of the important technologies for RON improvement in oil refining [5,10,11] and it is one of the largely used petrochemical processes. It is well known that low temperatures are preferred for alkane isomerization processes because the equilibria favors branched (high-octane-number) products [12], thus in order to achieve maximum isomer yields, the isomerization of *n*-paraffins must be carried out at the lowest possible temperatures over highly efficient catalysts [13]. Isomerization reactions are currently carried out very successfully using bifunctional supported platinum catalysts (reaction temperature 383–453 K [14]) [15–19]. Despite the higher yields of branched isomers owing to the lower temperatures of the process, these catalysts are very sensitive to poisons such as water or sulfur

* Corresponding author. Tel.: +213 7 73 21 39 69.
*E-mail address:* yacinereference@yahoo.com (Y. Rezgui).

0926-860X/$ – see front matter © 2008 Elsevier B.V. All rights reserved.
doi:10.1016/j.apcata.2008.04.038

compounds, and can cause corrosion and pollution problems [20,21]. In this mean it is of paramount importance to prepare and elaborate new environmentally benign catalysts which can replace these commercial catalysts (Pt supported on acidic alumina). In this respect, sulfated zirconia (SZ) was proposed as an alternative in isomerization processes [22]. Although the SZ catalysts have proved to be very active initially, they suffer from fast deactivation owing to reduction of sulfate groups, sulfur loss, and coke deposition. A solution to this problem has not yet been reported in the open literature [11]. Consequently, more active catalysts are needed that can operate at low temperatures while being environmentally friendly. Extensive research has been done in the search for such catalysts [23]. To contribute to this field, our group has proposed the use of nickel-tungsten based catalysts; however the collected data showed that the rate of hydrogenolysis reactions on these materials was high which leaded to a decrease in isomer yields [24,25]. Based on the fact that the performance of the doubly promoted catalyst shows further improvement in catalytic activity, stability, and selectivity of iso-alkane over the singly promoted catalyst in *n*-alkane isomerization reaction [26], we have tried to incorporate platinum to our Ni-W based solids.

The preparation method of catalysts is as important as the chemical composition; it determines not only the initial dispersion but also the metal–support interaction. This interaction may modify the acid sites of the support and the electronic properties of the metal [27,28]. Besides, it is well established that a calcination step, prior to the catalyst reduction, is needed in order to stabilize the catalyst. Such relatively high-temperature treatment of the catalyst may have an effect on both the metal function (metal sintering [29]) and the acid function (dehydroxylation of Brönsted sites). The reduction step strongly influences the final particle size of the active metal [27]. Accordingly, to manufacture catalysts in an efficient and reproducible process, it is essential to gain the control over these parameters. Several types of preparation techniques have been reported in the literature: mechanical mixing of metal compound and support, ion exchange processes, coprecipitation of metal oxides and support, impregnation and incipient wetness processes [30–32], solid–solid wetting [33], grafting of metal alkoxide precursors onto a metal oxide support alkoxides [34,35] and sol–gel procedure [36,37]. Taking into account all these facts, the objective of our research was the incorporation, by different methods, of platinum in Ni-$WO_x$/$SiO_2$-$Al_2O_3$ catalysts and the attempt to study the effect of pretreatment conditions on the activity of the prepared solids.

This study is a continuation of our earlier work [38] on Ni-Pt-W based solids. We reported in Part 1 that the activities as well as the density of acid sites of the catalysts prepared by a sol–gel method noted $(Ni_xPt_y)_{BC}$, where the platinum was incorporated before calcination, depend strongly on their calcination temperature and that the reducibility of these samples do not exhibit the PtO reduction peak, this behavior was ascribed to the platinum-tungsten interaction, which was dependent on the pretreatment conditions. The aim of this study is to investigate $(Ni_xPt_y)_{AC}$ catalysts, prepared by a hybrid method, sol–gel and incipient wetness, where the platinum was incorporated after calcination, to quantify and relate their catalytic performance with their pretreatment conditions.

## 2. Experimental

### 2.1. Catalyst preparation

A series of nine catalysts noted $(Ni_xPt_y)_{AC}$ where *x* and *y* indicate the percentage of nickel and platinum in the catalyst (Table 1), and AC indicate that the incorporation of Pt was done after calcination, having the same amount of tungsten (10%) and a constant $SiO_2/Al_2O_3$ ratio (1.83), was prepared by using an hybrid method: sol–gel and incipient wetness impregnation. A sol was obtained by mixing, under vigorous stirring, an aqueous solution of nickel nitrate ($Ni(NO_3)_2{\cdot}6H_2O$) preliminarily acidified by nitric acid with the required amounts of aluminum sulfate ($Al_2(SO_4)_3{\cdot}18H_2O$) and sodium tungstate ($Na_2WO_4$). To the sol obtained, under vigorous stirring, an aqueous solution of sodium silicate ($Na_2SiO_3$) was added. To exchange undesirable ions, such as $Na^+$, the prepared gel was activated, under reflux conditions in a thermostat, with ammonium sulfate (liquid to solid ratio of 30) at 60 °C over a period of 48 h (this unit operation was repeated several times), washed with hot water (60 °C), dried at 120 °C for 4 h and finally calcined at 500 °C for 5 h. A heating rate of 10 °C/min was used. After calcination, the obtained solids were impregnated with a solution of hexachloroplatinic acid containing the appropriate concentration of Pt, the time of impregnation was 6 h. The samples thus prepared were dried at 120 °C overnight and calcined in the temperature range 300–700 °C for 5 h. A heating rate of 10 °C/min was used.

**Table 1**
Physico-chemical properties of the $(Ni_xPt_yW/ASA)_{AC}$ samples (noted $(Ni_xPt_y)_{AC}$)

| Catalyst | % Ni | | % Pt | | % W | $SiO_2/Al_2O_3$ |
|---|---|---|---|---|---|---|
| | Theoretical | Practical | Theoretical | Practical | | |
| $(Ni_{12}Pt_0)$ | 12 | 12.00 | 0.0 | 0.00 | 10 | 1.83 |
| $(Ni_{12}Pt_{0.1})_{AC}$ | 12 | 12.00 | 0.1 | 0.10 | 10 | 1.83 |
| $(Ni_{12}Pt_{0.4})_{AC}$ | 12 | 12.00 | 0.4 | 0.39 | 10 | 1.83 |
| $(Ni_{12}Pt_1)_{AC}$ | 12 | 11.96 | 1.0 | 0.98 | 10 | 1.83 |
| $(Ni_{15}Pt_0)$ | 15 | 14.96 | 0.0 | 0.00 | 10 | 1.83 |
| $(Ni_{15}Pt_{0.1})_{AC}$ | 15 | 14.94 | 0.1 | 0.1 | 10 | 1.83 |
| $(Ni_{15}Pt_{0.4})_{AC}$ | 15 | 14.96 | 0.4 | 0.38 | 10 | 1.83 |
| $(Ni_{15}Pt_1)_{AC}$ | 15 | 14.96 | 1.0 | 0.99 | 10 | 1.83 |
| $(Ni_{17}Pt_0)$ | 17 | 16.90 | 0.0 | 0.00 | 10 | 1.83 |
| $(Ni_{17}Pt_{0.1})_{AC}$ | 17 | 16.85 | 0.1 | 0.09 | 10 | 1.83 |
| $(Ni_{17}Pt_{0.4})_{AC}$ | 17 | 16.85 | 0.4 | 0.38 | 10 | 1.83 |
| $(Ni_{17}Pt_1)_{AC}$ | 17 | 16.87 | 1.0 | 0.98 | 10 | 1.83 |

For comparison purposes, Pt-free catalysts containing 12, 15, 17% Ni and 10% of tungsten supported on amorphous silica-alumina were prepared as described in Refs. [39,40].

### 2.2. Catalyst characterization

The nitrogen physisorption measurements were performed at the temperature of liquid nitrogen (77 K) and the specific surface areas of the catalysts were calculated using the BET method. Prior to measuring the adsorption, all samples were degassed at 350 °C for 30 min, and then reduced at 430 °C, with hydrogen, for 1 h.

The samples were digested with mixed acids, and their chemical compositions were determined by inductively coupled plasma-atomic emission spectroscopy (ICP-AES).

The relative differences in the reducibility of the prepared catalysts, related to the oxidation state, dispersion, and metal–support interaction, were studied by means of temperature-programmed reduction (TPR) by hydrogen using an Ohkura TP 2002 S equipped with a thermal conductivity detector. Initially samples were exposed at 500 °C to an air flow for 3 h and subsequently cooled to room temperature. Next, they were analyzed with a reducing gas $Ar/H_2$ (95/5 volumetric ratio) in the temperature range 100–600 °C, heating at 5 °C/min.

The acidity of the catalysts was measured by ammonia thermal-programmed desorption (TPD of $NH_3$). Prior to TPD experiments, all the samples were treated in situ in an oxygen flow at 500 °C for 3 h, then outgassed in helium flow at 300 °C, and finally reduced in hydrogen flow at 430 °C for 2 h. After reduction, the sample was further dried in flowing He at 300 °C for 1 h and then cooled to

room temperature. When the system became steady, ammonia was passed at 100 °C for 30 min (using a 10% $NH_3$/He carrier gas). The samples were then purged, at the same temperature, with helium flow (100 ml/min) for 1 h. The TPD spectrum was obtained by heating the sample from 100 °C to 700 °C at a heating rate of 10 °C/min under a He flow. Ammonia desorption was continuously measured by means of thermal conductivity detector, and the water evolved was trapped in a KOH trap located immediately before the TCD.

### 2.3. Catalytic test

The catalytic experiments were performed in a continuous flow fixed-bed quartz reactor, loaded with 1 g of the catalyst, operated under isothermal conditions, and heated by a controlled temperature electrical oven. The *n*-hexane conversion was studied at atmospheric pressure, 250 °C, weight hourly space velocity (WHSV) = 4 $h^{-1}$ and a molar ratio of hydrogen/hydrocarbon ($H_2$/*n*-hexane) = 5.

The reaction products were analyzed on-line by gas chromatography.

Catalytic activity is expressed in term of conversion, which is defined as the fraction of the *n*-hexane which has reacted, whereas isomerization selectivity was defined as the yield of $C_6$ isocomponents divided by *n*-$C_6$ conversion.

## 3. Results and discussion

### 3.1. Chemical composition

Table 1 summarizes the theoretical and practical chemical composition of the prepared solids. From the collected data, it can be said that the practical chemical compositions were slightly lower than the theoretical ones, especially for catalysts with 17% Ni, which means that there was a loss in nickel and platinum during the preparation and treatment procedures.

### 3.2. BET surface area

Fig. 1 gives the evolution of the BET surface area of the prepared samples with their calcination temperature. The results show clearly that regardless the nickel and platinum amounts, the BET surface area of the $(Ni_xPt_y)_{AC}$ samples increased with increasing calcination temperature, passed through a maximum then decreased. The phenomenon being dependent on nickel and platinum contents; the higher the platinum amount the lower the calcination temperature at which the maximum BET surface area was obtained. Besides, for Pt-doped catalysts, the higher the nickel amount the lower the value of the BET surface area.

### 3.3. Acidity

The acid strength and concentration of the prepared catalysts are detected by the temperature and amount of ammonia desorption from their $NH_3$ adsorbed samples measured by TPD with on-line titration and displayed in Fig. 2. The results show that the acidic properties of the prepared samples may be considerably modified by varying the pretreatment conditions. From Fig. 2(a) which displays the dependence of the weak acid sites concentration of the most important prepared samples on their calcination temperature, it can clearly be seen that, whatever the nickel and platinum loadings, the weak acidity, peak desorption temperature in the TPD curve (not shown) ranging from 130 °C to 220 °C, increased with calcination temperature, passed through a maximum then decreased. In addition, for the same Pt content this acidity was enhanced by a rise in Ni loading till a maximum at 15% Ni then it decreased, whereas increasing the platinum concentration induced a decrease in the calcination temperature showing the maximum of the weak acidity. Besides, the effect of platinum on the density of the weak acid sites was dependent on nickel concentration, for samples with 12% Ni, the Pt addition leaded first to a rise in weak acidity then to a decrease, while for materials with 15 and 17% Ni, the weak acid sites concentration was enhanced by

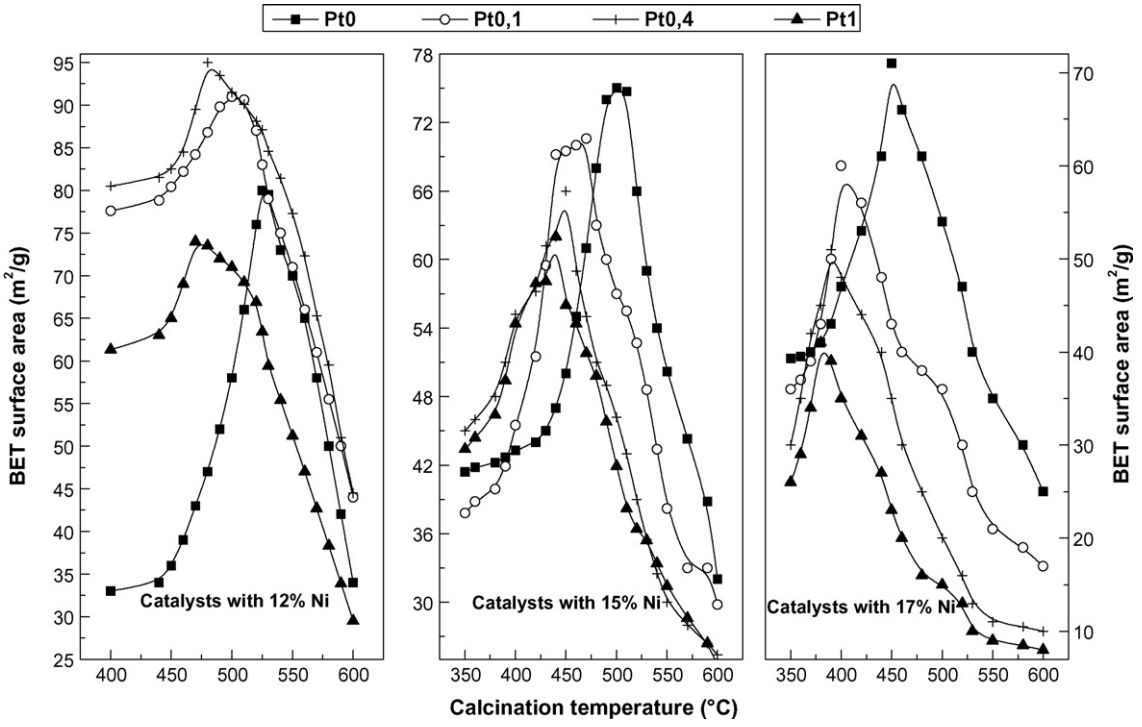


**Fig. 1.** Dependence of the BET surface area of the prepared catalysts on their calcinations temperature.

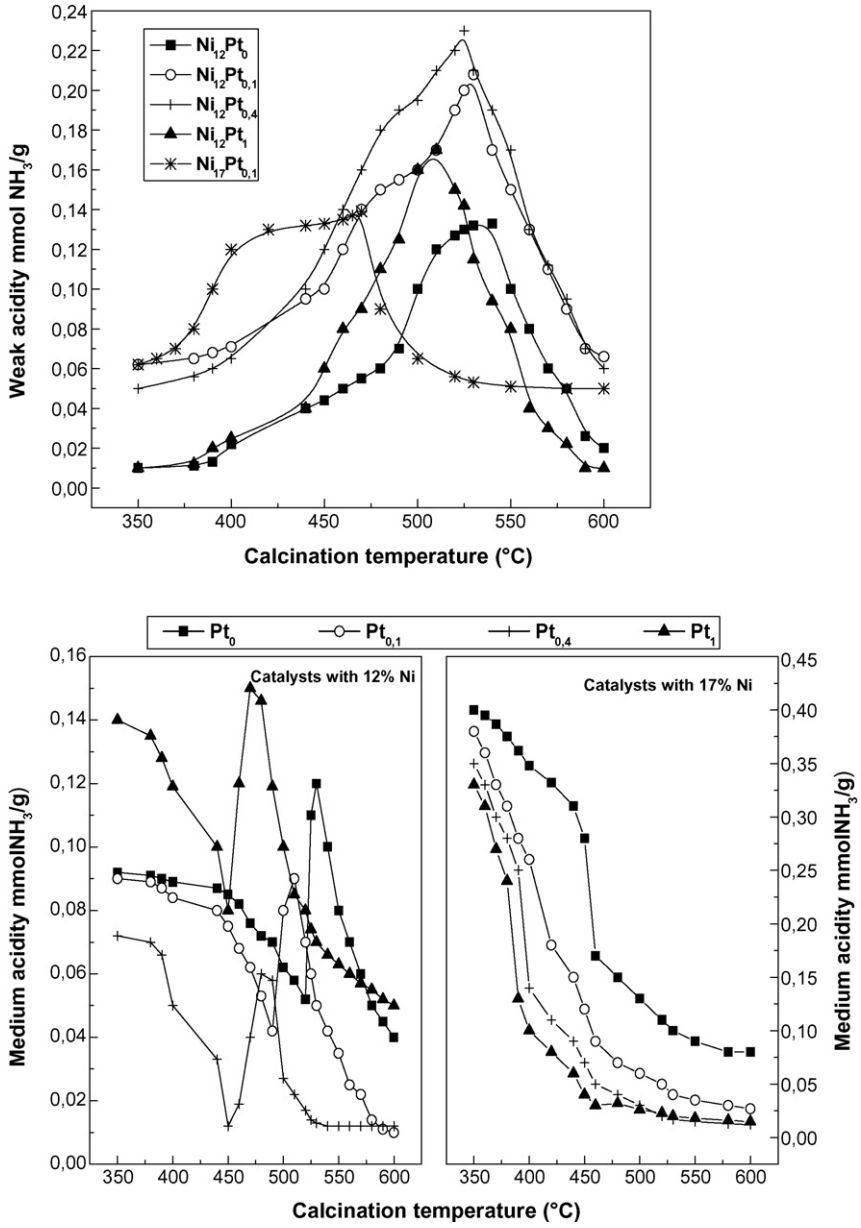


**Fig. 2.** (a) Dependence of the weak acid sites concentration of the prepared catalysts on their calcination temperature. (b) Dependence of the medium acid sites concentration of the prepared catalysts on their calcination temperature.

a rise in platinum loading. This infers that nickel and platinum as well as calcination at lower temperature generate acid sites of lower acidity. Similar results were reported by Boskovic et al. [41] during their study on the *n*-hexane isomerization over Pt-Na(H)Y catalysts. According to the open literature, these results may be explained by the formation of $Pt(OH)^{+}$ in the Brönsted acid sites which can account for the lower strong acidity shown by the catalysts [28], or by the fact that platinum activates hydrogen and the hydrocarbon and create Brönsted acid sites and carbenium ions [42], this was inferred from the ability of the tungstate species, which are present at intermediate coverage, to form $W^{5+}OH$ groups under reducing conditions. Furthermore, the results found in the case of $(Ni_{12}Pt_1)_{AC}$ catalyst may be explained by the fact that these latter species ($W^{5+}OH$ groups) were reduced to metallic tungsten at the optimum reduction temperature of this solid which leaded to a lowering in the number of weak acid sites. Finally, we have to mention that from Fig. 2(a), it is obvious that the week acidity plot has a similar shape and tendency to that obtained in Fig. 1 (BET plot), which means that the weak acidity tendency is due basically to the specific surface area modification.

On the other hand, from the dependence of the amount of medium acid sites, peak desorption temperature in the TPD curve (not shown) ranging from 300 °C to 320 °C, on the samples calcination temperature, it can clearly be seen from Fig. 2(b) that, in the case of catalysts with 12% Ni, regardless the platinum concentration, the number of medium acid sites decreased with calcination temperature to reach a minimum, then it was enhanced till a maximum and afterwards it decreased again by a rise in calcination temperature. It is noteworthy that the maximum location of the medium acid sites is shifted toward lower temperatures by increasing the platinum content. These results may be explained by the fact that calcination at lower temperature generates acid sites of lower acidity (Brönsted acid sites) and consequently the amount of medium acid sites will be

lowered. Besides, as mentioned by Romero et al. [43], with increasing calcination temperature, Lewis acid sites (strong sites) are formed as a result of dehydroxylation processes, thus the number of medium acid sites will be enhanced. Finally, a rise in the calcination temperature (above 500 °C) causes the increase of the crystallite size, as would be expected due to the major extension of sinterization, which leads to a partial block of the catalysts pores by large nickel particles that hinder the ammonia to enter them. Same results, concerning the decrease of stronger acid sites with calcination temperature, were reported by Romero et al. [44] during their study on the effects of the nickel incorporation method on the properties of bifunctional catalyst Ni/HZSM-5. In addition, the collected data show that, for catalysts with 15% Ni (solids with 17% Ni behave similarly), whatever the platinum loading, the increase of calcination temperature results in substantial drop of the amount of medium acid sites, the phenomenon is more noticeable for solids with 17% Ni. These results may be explained by the fact that in the case of samples with high nickel loading (15 and 17%), the calcination temperature leading to sinterization will be shifted toward lower temperatures and consequently the number of medium acid sites will be lowered. On the other hand and according to Jao et al. [21] and Lucas et al. [45], the decrease in the medium acid site density could be due to the acid sites to be partially covered by the metal particles.

### 3.4. Reduction behavior

The TPR profiles of the $(Ni_xPt_y)_{AC}$ catalysts are given in Fig. 3(a–c). As it can clearly be seen, the reduction profiles of $(Ni_xPt_y)_{AC}$ samples, characterized by multiple reduction peaks with poor resolution, evidence their complex reduction behavior. They exhibit a sharp peak which intensity is increasing with platinum loading; this increase is not proportional to the Pt content rise. The

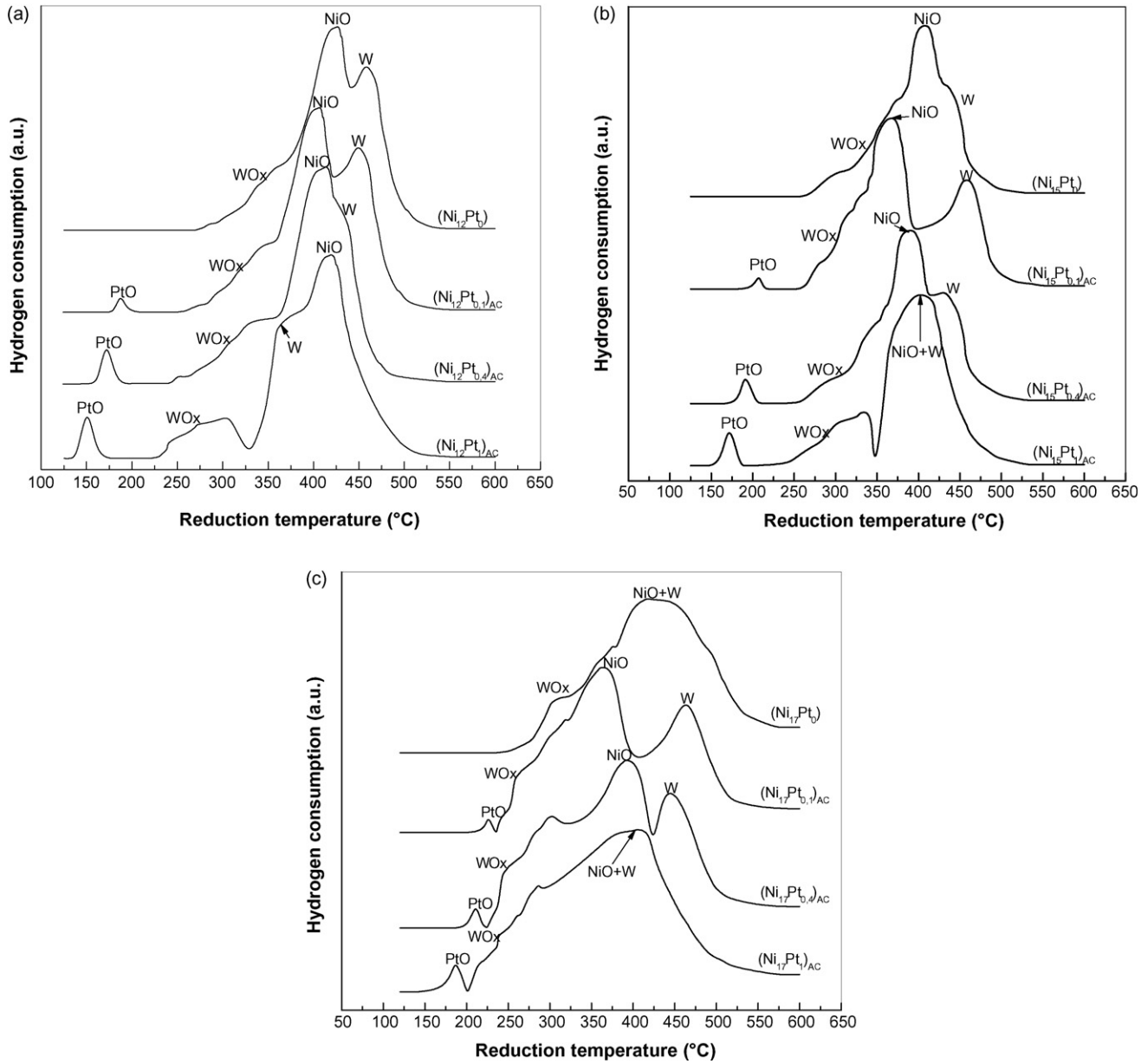


**Fig. 3.** (a) TPR profiles for $(Ni_{12}Pt_y)_{AC}$ samples calcined at their optimum calcination temperature. (b) TPR profiles for $(Ni_{15}Pt_y)_{AC}$ samples calcined at their optimum calcination temperature. (c) TPR profiles for $(Ni_{17}Pt_y)_{AC}$ samples calcined at their optimum calcination temperature.

peak maxima are shifting to higher temperatures with an increment in nickel content and toward lower values with increasing platinum concentration. This first hydrogen consumption is followed by a steady increase in the base line which is shifting to lower temperatures with increasing platinum concentrations. The increase in the base line is followed by either two peaks (the case of $(Ni_{12}Pt_{0,1})_{AC}$, $(Ni_{15}Pt_{0,1})_{AC}$, $(Ni_{17}Pt_{0,1})_{AC}$ and $(Ni_{17}Pt_{0,4})_{AC}$ catalysts) or a shoulder and a peak (the case of $(Ni_{12}Pt_{0,4})_{AC}$, $(Ni_{12}Pt_1)_{AC}$ and $(Ni_{15}Pt_{0,4})_{AC}$ catalysts) or a very large peak (the case of $(Ni_{15}Pt_1)_{AC}$ and $(Ni_{17}Pt_1)_{AC}$ catalysts). While the base line was shifted toward lower temperatures with increasing Pt content, the second peak maxima (NiO reduction peak) shifted toward lower values till 0.1% Pt then toward higher temperatures with a rise in platinum amount, whatever the nickel content. Furthermore with an increment in Pt concentration, the third peak maxima ($WO_x \rightarrow W$ peak) was shifted to lower temperatures in the case of $(Ni_{12}Pt_y)_{AC}$ solids, whereas its position shifted to higher temperatures till 0.1% Pt then toward lower values with increasing Pt for the other $(Ni_xPt_y)_{AC}$ ($x \neq 12$) samples.

In a previous paper [39], we have reported that, in the case of Pt-free catalysts (Ni-$WO_x$/$SiO_2$-$Al_2O_3$ solids noted ($Ni_xPt_0$)), the $H_2$-TPR spectra appear as a combination of the corresponding monometallic (Ni/$SiO_2$-$Al_2O_3$ and $WO_x$/$SiO_2$-$Al_2O_3$ materials) spectra, although they present some differences; they display small shifts of the tungsten species hydrogen consumption maxima toward lower temperatures and of the nickel species reduction peak toward higher temperatures. In addition, we have also ascribed the increase in the base line to the reduction of tungsten oxide species of various reducibilities, while the low-temperature peak was assigned to the reduction of the nickel oxide and the high-temperature peak was ascribed to a further reduction of the tungsten oxide species. In the case of ($Ni_{17}Pt_0$), the large peak was the result of the superimposition of two reduction peaks, the first of the NiO and the second of the $WO_x$ species. Based on these observations and on the maxima of TPR peak values given in Table 2 as well as on the finding of Wong et al. [26] who mentioned that platinum reduction usually occurs at a temperature between 100 °C and 200 °C, we can establish that the first peak can be clearly ascribed to the reduction of platinum oxide "PtO" [46,47]. This low reduction temperature, when compared to other catalysts [48], indicates a low Pt-$WO_x$ or Pt-support interaction, same observations were reported by Vaudagna et al. [49] in the case of $WO_x$-$ZrO_2$ and Pt/$WO_x$-$ZrO_2$ catalysts. As mentioned above, this peak is shifting to higher temperatures with an increment in nickel content, which infers that platinum reduction occurs hardly in the presence of nickel, this phenomenon could be related to the Pt-$WO_x$ interaction and to the fact that nickel ameliorates the tungsten dispersion. Thus, with increasing Ni content, the tungsten will be well dispersed and consequently the platinum-tungsten interaction will be stronger and the Pt reduction peak will shift toward higher temperatures. In contrast, the peak shifted toward lower temperatures with a rise in Pt content which suggest that Pt reduction occurs more readily in solids with less dispersion.

Based on the observations quoted in the previous section, the increase in the base line could be assigned to the reduction in several steps of $WO_x$ species, the second peak to the reduction of the nickel oxide and the third maxima to a further reduction of the tungsten oxide species. As earlier mentioned, the base line was shifted toward lower temperatures with increasing Pt content which indicates a platinum reduction catalytic action. Similar results were reported by Drago and Kob [50] during their study on the acidity and reactivity of sulfated zirconia and metal-doped sulfated zirconia, where they have shown that, whereas the $W^{5+}$ signal of the tungsten phase appears only at reduction temperatures of 473 K on the unpromoted WZ catalyst, it appears on the promoted PtWZ catalyst already at room temperature, which lead them to conclude that promotion by platinum has a significant effect on the reducibility of the surface tungstate phase of the catalyst by $H_2$. In addition, Kuba et al. [23] have mentioned, during their study on the structure and properties of tungstated zirconia catalysts, that the addition of platinum leads to lower reduction temperatures, evidently because of spillover of hydrogen adatoms (formed by $H_2$ dissociation on platinum) onto condensed $WO_x$ clusters.

On the other hand and as earlier mentioned whatever the nickel content, the NiO reduction peak position was shifted toward lower values till 0.1% Pt then toward higher temperatures with a rise in platinum amount. As mentioned by Telkar et al. [51], the addition of platinum to Pt-free solids leads to the stabilization of $Ni^0$ state under reducing conditions, which is probably the cause of lowering the value of the NiO TPR-peak maxima. Besides, the NiO TPR-peak maxima shift toward higher temperatures could be explained by the combination of two factors; the synergism between Pt-$WO_x$ and Ni-$WO_x$ interactions and the amelioration of tungsten dispersion by nickel. At higher nickel loading and lower platinum content, tungsten and platinum are well dispersed, thus the Pt-$WO_x$ interaction is so strong so as that the Ni-$WO_x$ interaction will be weakened and the NiO peak shift toward lower temperatures will be more marked. With increasing Pt content, the Pt-$WO_x$ interaction will be weakened and the peak shift will be less noticeable (see Fig. 4a: $S_1(425 - 365 = 60\,^{\circ}C) > S_2\,(425 - 395 = 30\,^{\circ}C) > S_3\,(425 - 405 = 20\,^{\circ}C)$ for samples with 17% Ni and $S'_1(410 - 370 = 40^{\circ}C) > S'_2(410 - 390 = 20^{\circ}C) > S'_3(410 - 404 = 6^{\circ}C)$ for solids with 15% Ni). Moreover, at lower nickel concentrations (12%), the tungsten is less dispersed and consequently the Pt-$WO_x$ interaction will be less effective especially for 1% Pt (Fig. 4a:

**Table 2**
TPR peak maxima and optimum calcination temperatures for the $(Ni_xPt_y)_{AC}$ catalysts

| Catalyst | Optimum calcination temperature (°C) | TPR peak maxima and increase in base line | | | |
|---|---|---|---|---|---|
| | | Increase in the base line (°C) | First peak (°C) | Second peak or shoulder (°C) | Third peak or shoulder (°C) |
| $(Ni_{12}Pt_0)$ | 525 | 280–370 | / | 420 | 460 |
| $(Ni_{12}Pt_{0,1})_{AC}$ | 500 | 265–358 | 195 | 400 | 450 |
| $(Ni_{12}Pt_{0,4})_{AC}$ | 480 | 250–355 | 185 | 410 | 430 (shoulder) |
| $(Ni_{12}Pt_1)_{AC}$ | 470 | 232–307 | 162 | 365 (shoulder) | 418 |
| $(Ni_{15}Pt_0)$ | 500 | 265–375 | / | 410 | 440 (shoulder) |
| $(Ni_{15}Pt_{0,1})_{AC}$ | 460 | 260–340 | 207 | 370 | 460 |
| $(Ni_{15}Pt_{0,4})_{AC}$ | 450 | 251–360 | 194 | 390 | 430 (shoulder) |
| $(Ni_{15}Pt_1)_{AC}$ | 440 | 230–340 | 172 | 404 (large peak) | / |
| $(Ni_{17}Pt_0)$ | 450 | 260–375 | / | 425 (large peak) | / |
| $(Ni_{17}Pt_{0,1})_{AC}$ | 400 | 258–318 | 228 | 365 | 465 |
| $(Ni_{17}Pt_{0,4})_{AC}$ | 390 | 252–316 | 212 | 395 | 445 |
| $(Ni_{17}Pt_1)_{AC}$ | 380 | 225–294 | 190 | 405 (large peak) | / |

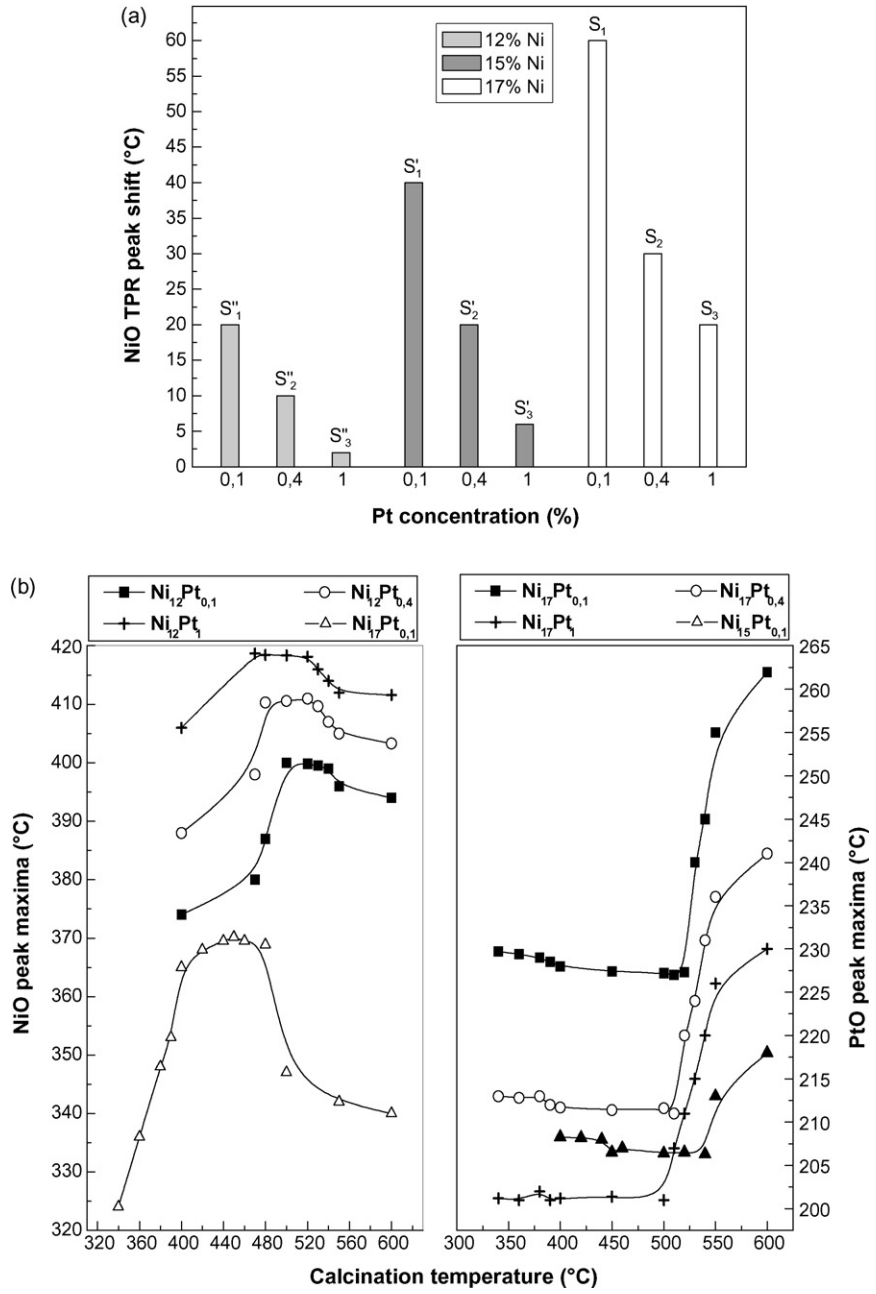


**Fig. 4.** (a) Variation of NiO reduction peak shift with Ni and Pt concentrations. (b) Variation of PtO and NiO reduction peak positions with the calcination temperature.

$S''_3 = 420 - 418 = 2\,^{\circ}C$). In addition it was earlier mentioned that the third peak ($WO_x \rightarrow W$) was shifted to higher temperatures till 0.1% Pt then toward lower values with increasing Pt for the other $(Ni_xPt_y)_{AC}$ ($x \neq 12$) samples. The phenomenon could be explained by the combination of two factors, the Pt-$WO_x$ interaction which is translated by the $WO_x$ peak shift to higher temperatures and the $WO_x$ reduction catalyzed by hydrogen spillover caused by platinum which is translated by the $WO_x$ peak shift toward lower temperatures. At higher nickel loading and less platinum concentrations, the first effect (Pt-$WO_x$ interaction) is more pronounced, with decreasing Ni and increasing Pt, especially for $(Ni_{12}Pt_1)_{AC}$, the latter effect (hydrogen spillover) will be more noticeable at the detriment of the first one.

Concerning the variation of the NiO reduction peak with calcination temperature, the collected data (the most relevant results are shown in Fig. 4b) show that all samples displayed virtually identical trends with increasing calcination temperature, in that the NiO peak is initially shifted toward higher temperatures, then its position becomes nearly constant and finally it shifts toward lower temperatures. The phenomena being dependent on nickel and platinum amounts, the higher the nickel and platinum loadings the lower the calcination temperature at which the position of the NiO peak reaches its maximum value. This finding may be explained by the fact that the reduction of the large nickel particles and/or particles that interact weakly with the support is easier than the reduction of nickel that interacts strongly with the support [45]. Consequently the first particles type will display lower reduction temperature as compared to the latter one. In addition, larger nickel particles were formed when the nickel loading increased which lead to the weakening of the Ni-$WO_x$ interaction (the nickel-tungsten interaction is more noticeable when the two species are well dispersed) and to the boosting of the

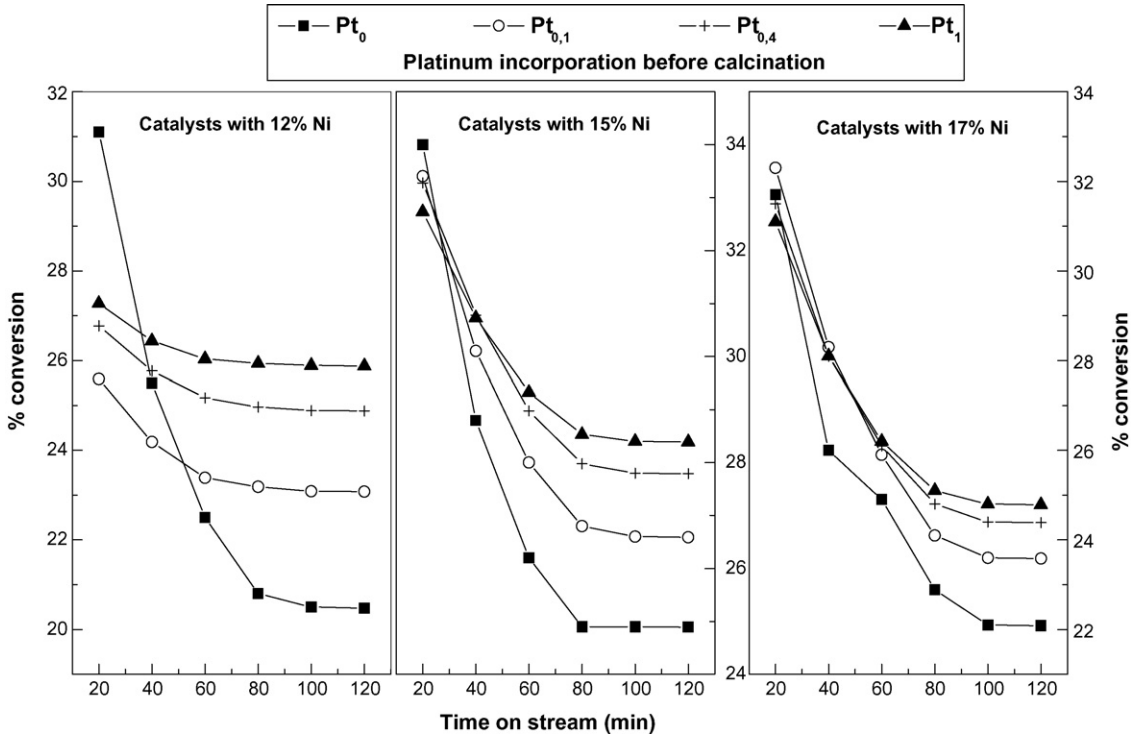


**Fig. 5.** Evolution of $(Ni_xPt_y)_{AC}$ catalysts activity with time on stream. Reaction temperature = 300 °C.

nickel hydrogenation ability. Consequently, dissociative $H_2$ chemisorption is easier on these large nickel particles. Since H atoms are better reducing agents than $H_2$ molecules, the large particles formed at high nickel content are reduced at lower temperatures.

Concerning the dependence of the PtO reduction peak on the samples calcination temperature, the collected data (Fig. 4b) show that whatever the calcination temperature, the PtO peak location is nearly constant for catalysts with 12% Ni, whereas for solids with 15 and 17% Ni, the PtO peak location decreases slightly and then increases with increasing calcination temperature. The phenomenon being dependent on the platinum concentration, the higher the platinum content the lower the calcination temperature at which the PtO reduction peak position begins to shift toward higher temperatures. The results found in the case of $(Ni_{12}Pt_y)_{AC}$ solids, may be related to the fact that a rise in calcination temperature induces a well dispersion of nickel and platinum. However, the dispersion of nickel induces a lowering in Pt-W interaction, whereas the platinum dispersion leads to an enhancement in Pt-W interaction. Thus, the balance between the two effects will govern the reduction of platinum. Since for catalysts with 12% Ni the peak reduction remains constant, the two effects are well balanced. For solids with 15 and 17% Ni, the first stage will be explained by the Ni-W and Pt-W interaction balance, while the second stage (the shift of the PtO reduction peak toward higher values) may be assigned to the fact that the higher calcination temperatures lead to the sintering of nickel which is translated by a lowering of Ni-W thus Pt-$WO_x$ interaction effect will be more strong and more noticeable and the platinum reduction will occur hardly.

### 3.5. Performance in n-hexane hydroisomerization

#### 3.5.1. Evolution of catalytic activity with time on stream

Fig. 5 shows the dependence of $(Ni_xPt_y)_{AC}$ samples catalytic activity, expressed as the total conversion of *n*-hexane, on time on stream (TOS) at atmospheric pressure, at a reaction temperature of 300 °C and with the following operating conditions: $H_2/n\text{-}C_6 = 5$; weight hourly space velocity (WHSV) = 4 $h^{-1}$. This dependence was studied at samples optimum reduction and calcination temperatures. Conversions changed with time on stream and the same qualitative pattern was observed for each catalyst. The data indicate a period of declining conversion followed by a period of stabilization. Besides, the deactivation rates were higher with Pt-free catalysts than with the promoted ones due to deactivation by coking [25]. On the other hand, from the collected data it can be clearly seen that the incorporation of platinum produced, in the case of solids with 12 and 15 wt.% Ni, a large increase in steady state conversion and a small decrease in the deactivation rate, while it produced a noticeable decrease in stability for samples with 17 wt.% Ni. The colleted data infer that the deactivation rate is related to the density of medium acid sites. The $(Ni_{17}Pt_y)_{AC}$ catalysts, with the highest number of medium acid sites (from 0.28 to 0.33 mmol $NH_3$/g), display much higher deactivation as compared to $(Ni_{12}Pt_y)_{AC}$ having the lowest amount of medium acid sites (from 0.12 to 0.15 mmol $NH_3$/g). Besides for catalysts having the same number of medium acidity, the deactivation rate increased with increasing the Pt content. This observation rules out the dependence of the catalysts stability on the density of acid sites, nickel and platinum content. Thus, the deactivation may be due to a metallic function poisoning, or to a loss of the support acidity, or finally, to a loss of the hydrogen dissociation capacity of $WO_x$ species, which is rapidly deactivated by coke [52].

#### 3.5.2. Effect of calcination temperature

Fig. 6(a) shows changes, over the most important prepared samples, of *n*-hexane conversion over $(Ni_{12}Pt_y)_{AC}$ solids (the other prepared materials show almost identical trends), as a function of calcination temperature at a reaction temperature of 250 °C, a time on stream of 100 min and at different reduction temperatures (260 °C and optimal reduction temperatures at which the three oxides (PtO, $WO_3$ and NiO are reduced)). From the collected data it can be said that regardless the reduction temperature as well as the

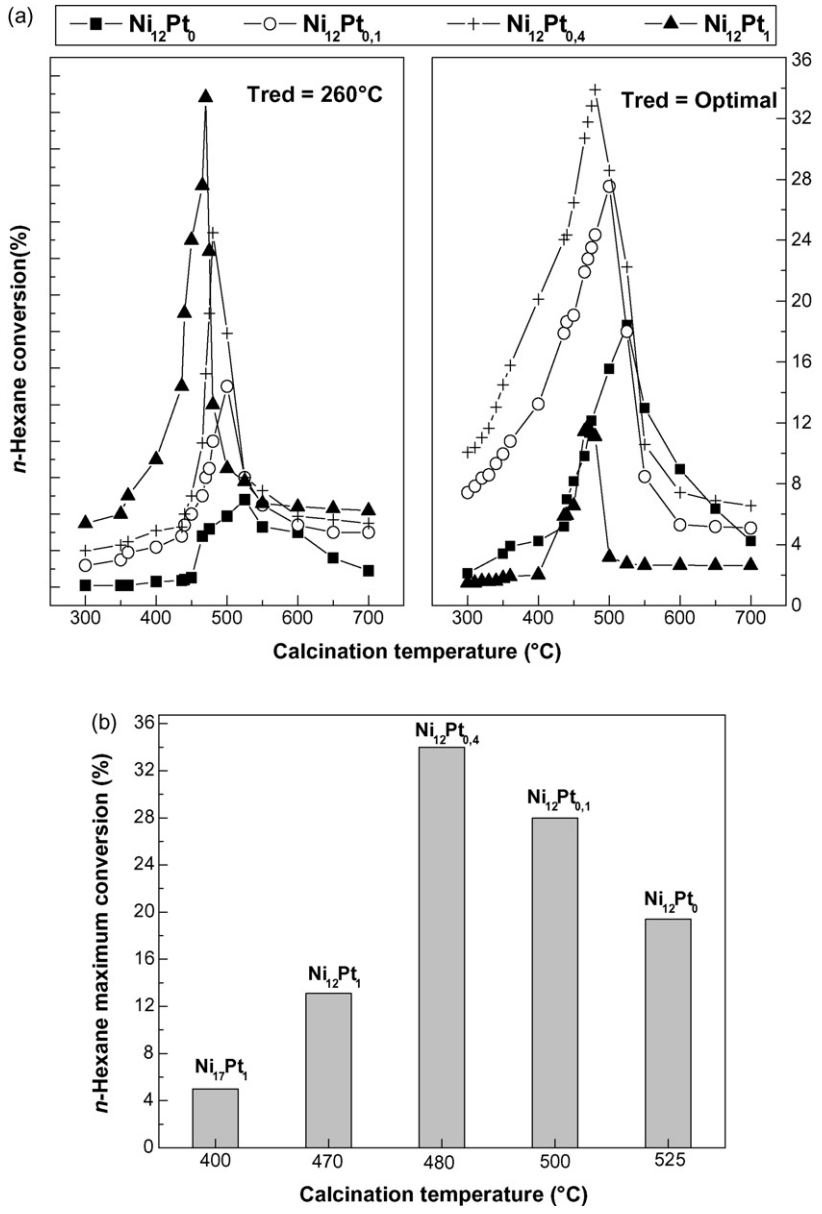


**Fig. 6.** (a) Effect of calcination temperature on the performance of $(Ni_{12}Pt_y)_{AC}$ catalysts. Treac = 250 °C and time on stream (TOS) = 100 min. (b) Effect of Ni and Pt loadings on the position of *n*-hexane maxima conversion. Reaction temperature = 250 °C, reduction temperature = optimal, TOS = 100 min.

Ni and Pt contents, all the prepared catalysts display similar behaviors in that their catalytic activity increased with calcination, passed through a maximum and then decreased. Calcination at 700 °C yielded the lowest activity. Besides, the calcination temperature that gave the highest activity was different for each sample, the lower the nickel and platinum amounts the higher the calcination temperatures showing the maximum activity (Fig. 6b). These observations suggest that the catalyst activities depend strongly on the calcination temperature, reduction temperature as well as on the nickel and platinum concentrations. In addition, the shift of calcination temperature toward higher values with a decrease in Ni and Pt amounts may be related to the interaction of these metals with the support surface which is strong when the active species are present in small amounts, similar observations were previously reported by our group [38] during the study of the effects of pretreatment conditions on the catalytic performance of Ni-Pt-W/$SiO_2$-$Al_2O_3$ samples prepared by a sol–gel method and by Hino and Arata [53] during their study on the isomerization of *n*-butane over ($WO_3/ZrO_2$ + $Pt/ZrO_2$) catalysts. Besides, the collected data show clearly that the platinum incorporation affects differently the samples catalytic performance expressed as *n*-hexane conversions. The phenomenon being dependent on the catalysts composition as wall as on their reduction temperature, for samples reduced at 260 °C (Fig. 5a), whatever the nickel amount, a rise in Pt content induces a markedly increase in the catalytic activity of the prepared solids which infers that the incorporation of platinum on catalysts produces a beneficial effect since it reduces the rate of deactivation and consequently increases the catalyst activity. Similar observations on the beneficial effects on the catalysts activities were reported in the case of zeolites [54–57] and of sulfated or tungstated zirconia based solids [5,11,13,58–65] catalysts where it was confirmed that platinum was effective in preventing deactivation and consequently in enhancing catalyst activity. However, it is noteworthy that the results displayed in Fig. 5(a) may lead to wrong conclusions on the influence of platinum on the activity of the catalysts because at this reduction

temperature (260 °C) the nickel oxide was not reduced. Thus, it is interesting to compare the effect of platinum incorporation on the catalytic performance for samples reduced at their optimal reduction temperatures (temperatures at which PtO, $WO_3$ and NiO were reduced). At these reduction temperatures, the results displayed in Fig. 5(b) showed that the nickel content played an important role in determining the effect of platinum addition. For materials with 12% Ni, the activity increased with increasing Pt content till 0.4% and then decreased, while solids with 15 and 17% Ni behaved similarly in that their activities decreased with a rise in platinum amount, the effect being more noticeable for the latter samples. In previous papers [25,39], we have demonstrated that in the case of Pt-free catalysts ($Ni_xPt_0$), the amount of nickel giving the optimal metal-acid balance was 15%, thus if the metallic function is lower or higher than this value the catalytic performance will be lowered. This finding lead to the fact that the Pt-doped catalysts can be divide into two groups, the fist one containing the solids with 12% Ni and the second one containing the materials with 15 and 17% Ni. For the first group, the nickel value is less than the value giving the optimal metal-acid balance, thus increasing Pt content from 0 to 0.4% will lead to an enhancement in the metallic value and consequently to an enhancement in the catalytic performance, a further increase in Pt content (1%) caused a strong boosting in the metallic value so as the catalytic activity will be lowered. For samples with 15 and 17% Ni, the platinum addition will increase the metal content value than the ideal one and consequently the catalytic activity will be decreased.

Hereafter and for labeling purposes, we specify the wt.% of either Ni or Pt immediately after the chemical symbol as subscripts, and the optimum calcination temperature (in °C) (see Table 2) as the label suffix. For example, the 12 wt.% Ni and 0.1 wt.% Pt catalyst that had been calcined at 500 °C was labeled as $(Ni_{12}Pt_{0,1})_{AC}$-500.

### 3.5.3. Effect of reduction temperature

The dependence of the prepared samples activities on their reduction temperature was studied at 250 °C at their optimum calcination temperature and over duration of 100 min. As it can clearly be seen from the collected data displayed in Fig. 7 for $(Ni_{12}Pt_y)_{AC}$ catalysts (the other prepared samples behave similarly), except for the $(Ni_{12}Pt_1)_{AC}$ catalyst for which the activity increased with increasing the reduction temperature to reach a maximum, then it was decreased till a minimum, afterwards it raised to become finally constant, all the other prepared solids displayed the same trends regardless the Ni and Pt contents, in that their catalytic activities were boosted by a rise in the reduction temperature to reach a maximum or a plateau and afterwards decreased to become finally constant. The lowest activity was obtained at a reduction temperature of 600 °C, this may be ascribed to the fact that higher reduction temperatures induce a larger extent of undesirable tungsten (and support) reduction [46]. Besides, the optimum reduction temperature was shifted toward lower values with increasing Pt content, the effect being more pronounced when the nickel amount was higher.

If we recall the TPR profiles, these results may be interpreted by the presence of platinum and nickel having metallic properties and by reduced tungsten oxide species generated by hydrogen reduction, these reduced species being more active than the tungsten trioxide ($WO_3$) [47,48,66,67]. As mentioned by Drago and Kob [50], the higher reducibility of the tungstate phase due to platinum is potentially responsible for the strong enhancement of the catalytic activity and selectivity observed. Besides, the collected data may be ascribed to the synergism between nickel-tungsten and platinum-tungsten interaction. It is well known that the Pt-$WO_x$ interaction depends on the platinum and tungsten particle size, the smaller the particle size the stronger the Pt-$WO_x$ interaction and consequently the lower the Ni-$WO_x$ interaction, thus at lower platinum loading the Pt-$WO_x$ interaction is very strong, especially for solids with 17% Ni where the tungsten is well dispersed (small particle size). Or we have previously reported that the Ni-$WO_x$ interaction was translated by NiO reduction peak shift toward higher temperatures, thus if this interaction is weakened, the NiO reduction peak will shift toward lower temperatures and consequently do the optimum reduction temperature. The same result was reported by Larsen and Petkovic [46] with platinum supported on tungstated zirconia catalysts, and by Hua and Sommer [68] with alumina doped Pt/$WO_x$/$ZrO_2$ catalysts.

In addition, the results found in the case of the $(Ni_{12}Pt_1)_{AC}$ catalyst may be ascribed to the fact that the peak corresponding to the reduction WOx-W appeared before the NiO reduction peak thus we observed a minimum followed by an enhancement in the catalytic activity.

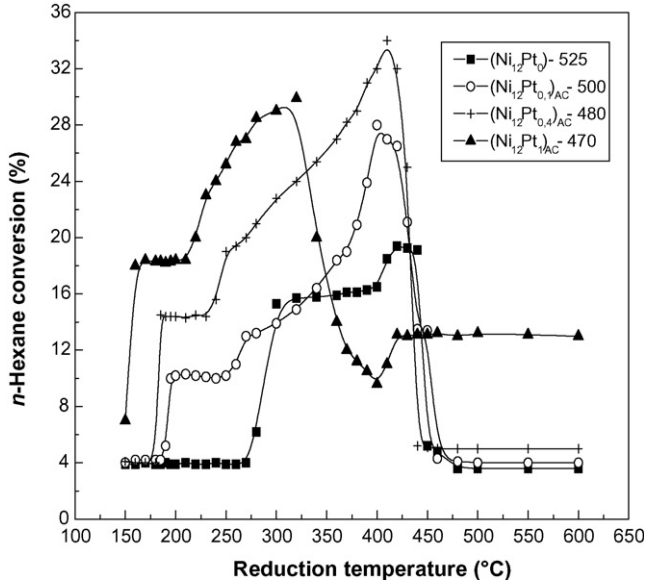


**Fig. 7.** Effect of reduction temperature on the performance of $(Ni_{12}Pt_y)_{AC}$ catalysts. Reaction temperature = 250 °C, calcination temperature = optimal, TOS = 100 min.

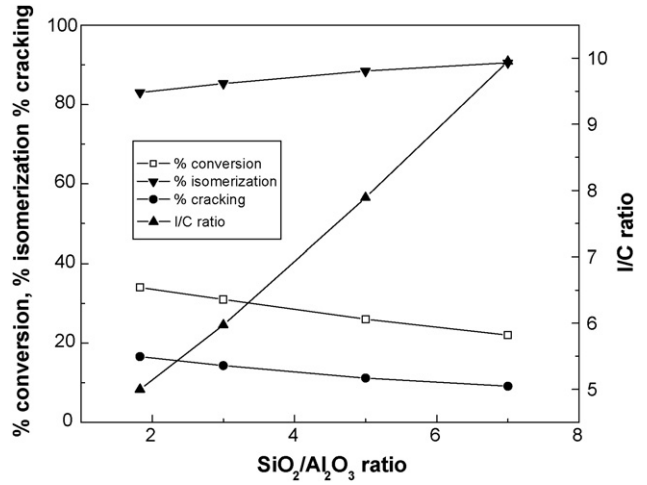


**Fig. 8.** Effect of $SiO_2/Al_2O_3$ ratio on *n*-hexane hydroconversion over $(Ni_{12}Pt_{0,4})_{AC}$ catalysts. Reaction temperature = 250 °C and TOS = 100 min.

Of the formulations screened in this work, the catalyst with 12 % of nickel and 0.4% of platinum $(Ni_{12}Pt_{0,4})_{AC}$ catalyst) showed by far the best performance. Thus, it is interesting to study in more details this system.

### 3.5.4. Effect of $SiO_2/Al_2O_3$ ratio

*n*-Hexane transformation over $(Ni_{12}Pt_{0,4})_{AC}$ catalysts with different $SiO_2/Al_2O_3$ ratios (1.83, 3, 5 and 7) at 250 °C is illustrated in Fig. 8. The higher the $SiO_2/Al_2O_3$ ratio the lower the activity and the higher the isomerization selectivity. In addition, the formation rate of cracking products decreases, while the I/C (isomerized to cracked products) ratio increases with increasing the Si/Al ratio. These effects may be explained by the fact that in catalysts with high $SiO_2/Al_2O_3$ ratios, the acid density is lower, so each intermediate olefin formed at a metallic dehydrogenating site comes into contact with very few acid sites between two metallic sites, which could favorably lead to the formation of isomerized products. In catalysts with lower $SiO_2/Al_2O_3$ ratios, each intermediate olefin comes into contact with more acid sites between two metallic sites and thus the cracking tendency clearly predominates.

### 3.5.5. Effect of $H_2/n\text{-}C_6$ molar ratio

The variation of *n*-hexane hydroconversion rate with hydrogen pressure was investigated at 250 °C by varying the hydrogen flow rate and keeping the partial pressure of *n*-hexane constant so that changing the $H_2/n\text{-}C_6$ molar ratio. The results are depicted in Fig. 9, where it can be seen that increasing the $H_2/n\text{-}C_6$ molar ratio from 5 to 15 decreased the conversion and increased the selectivity to isomers (I/C ratio increased). This behavior can be explained taking in account two factors. First, and as mentioned in a previous work [39] for Pt-free samples, the decrease in conversion was due to an increase in the overall $(H_2/n\text{-}C_6)$ space velocity, while the increase in the I/C ratio was due to the fact that isomerization reactions are faster than cracking reactions. Second, as cracking of isohexanes is faster than cracking of *n*-hexane, cracking reactions predominate at high conversions when isoproducts are present in large amounts. In the case of Pt-loaded catalysts, the same results were observed and thus they may be explained by the same facts.

### 3.5.6. Product distribution

Fig. 10 illustrates results of selectivity to isomerization products versus conversion over $(Ni_{12}Pt_{0,4})_{AC}$ catalyst at 250 °C and 100 min TOS. Monobranched isomers appear from low conversions and

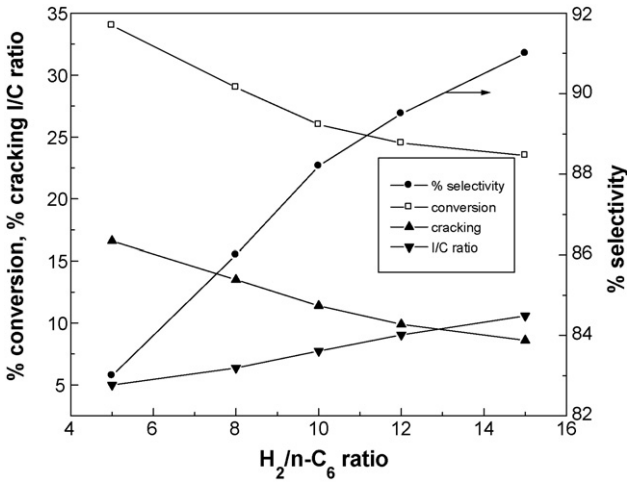


**Fig. 9.** Effect of hydrogen pressure on *n*-hexane hydroconversion over $(Ni_{12}Pt_{0,4})_{AC}$ catalysts. Reaction temperature = 250 °C and TOS = 100 min.

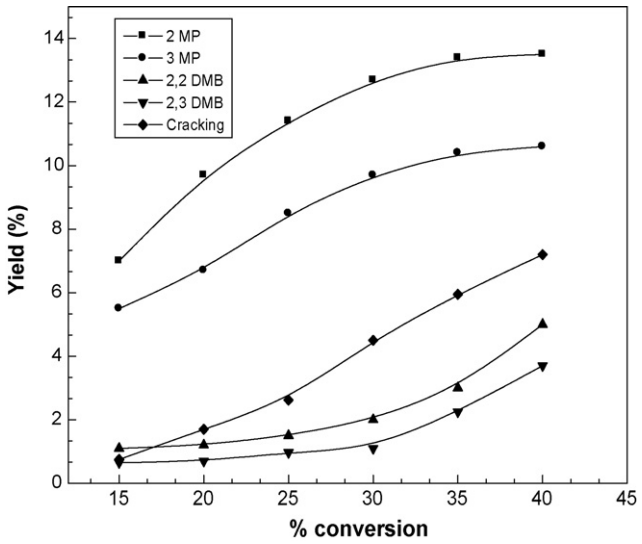


**Fig. 10.** Effect of conversion on *n*-hexane hydroconversion over $(Ni_{12}Pt_{0,4})_{AC}$ catalysts. Reaction temperature = 250 °C and TOS = 100 min.

their fraction increases up to a point where multibranched isomers and cracking products start to be significant (30% conversion). They dominate at all practical conversions and their formation increases together with that of multibranched isomers. On the other hand, the cracked products are not produced in significant amounts until about 30% conversion. These results infer that isomerization first leads to mono-branched isomers mainly then to multi-branched ones and that the formation of cracking products apparently succeeds the formation of branched isomers. Same results were reported by Roldan et al. [69] during their study on the influence of acidity and pore geometry on the product distribution in the hydroisomerization of light paraffins on zeolites, and by Pope et al. [70] during their study of catalysts formulations for isomerization of $C_7$ hydrocarbons.

## 4. Conclusion

The present investigation describes a new route to synthesize Pt-Ni-$WO_x/SiO_2$-$Al_2O_3$ catalysts. Our results show that the preparation method and the pretreatment conditions have a great influence over acidity, metal–support interaction and metal reducibility. The most outstanding observations are:

- Whatever the nickel and platinum contents, the BET surface areas of the catalysts prepared by the hybrid technique ($(Ni_xPt_y)_{AC}$ materials) increased with calcination temperature to reach a maximum then decreased, the phenomenon being dependent on nickel and platinum loadings. Whereas in the case of the samples prepared by the sol–gel method ($(Ni_xPt_y)_{BC}$ materials), the BET surface areas were not influenced by the calcination temperatures.
- As in the case of $(Ni_xPt_y)_{BC}$ solids, the activities of the $(Ni_xPt_y)_{AC}$ catalysts depend strongly on their calcination temperature; the incorporation of Pt shifts the optimum calcination temperature to lower values.
- The platinum incorporation affects differently the surface acidity of $(Ni_xPt_y)_{BC}$ and $(Ni_xPt_y)_{AC}$ samples.
- The reducibility of Pt-Ni-$WO_x$/ASA catalysts is very different whether the platinum was added before or after calcination. The $(Ni_xPt_y)_{BC}$ samples do not exhibit the PtO reduction peak, while the opposite feature is observed in the case of $(Ni_xPt_y)_{AC}$ solids.

This behavior was ascribed to the platinum-tungsten interaction, which is dependent on the preparative technique and on pretreatment conditions. The Pt-$WO_x$ interaction is much lower for $(Ni_xPt_y)_{AC}$ as compared to $(Ni_xPt_y)_{BC}$ samples.

- Comparing the maximum activity displayed by both series of catalysts, $(Ni_xPt_y)_{AC}$ samples exhibit much higher activities in *n*-hexane isomerization as compared to $(Ni_xPt_y)_{BC}$ catalysts and to Pt-free samples. Thus, it seems that platinum, added after calcination, is necessary to obtain the best catalytic activity.
- All catalysts deactivate with time on stream, with the conversion remaining steady after 100 min. The conversion drops severely in the case of Pt-free catalysts due to deactivation by coking and this activity drop is strongly temperature dependent. On the other hand, the stronger deactivation of cracking reactions compared to isomerization resulted in a net increase with TOS of hexane isomers. Moreover, the bimetallic samples show better stability when compared to Ni catalysts.
- For $(Ni_{12}Pt_{0,4})_{AC}$, the catalyst showing the best performance with a selectivity to isomers of 83% and a conversion of 34% at 250 °C, an increase in $SiO_2/Al_2O_3$ ratio induced a decrease in both conversion and cracking reactions, while selectivity to isomers as well as I/C ratio increase. In addition, it's suggested that the hydroisomerization selectivity of *n*-hexane is significantly affected by the hydrogen pressure.

## References


[1] R. Meusinger, Fuel 75 (1996) 1235.
[2] N. Viswanadham, B.S. Negi, M.O. Garg, M. Sundaram, B. Sairam, A.K. Agarwal, Fuel 86 (2007) 1290.
[3] T.G. Kaufmann, A. Kaldor, G.F. Stuntz, M.C. Kerby, L.L. Ansell, Catal. Today 62 (2000) 77.
[4] C. Marcilly, Stud. Surf. Sci. Catal. 135 (2001) 37.
[5] K. Watanabe, T. Kawakami, K. Baba, N. Oshio, T. Kimura, Catal. Surv. Asia 9 (2005) 17.
[6] C. Song, X. Ma, Appl. Catal. B 41 (2003) 207.
[7] I.V. Babich, J.A. Moulijn, Fuel 82 (2003) 607.
[8] J. Hancsók, S. Magyar, Z. Szoboszlai, D. Kalló, Fuel Process. Technol. 88 (2007) 393.
[9] I.H. Sven, Appl. Catal. 221 (2001) 421.
[10] P.J. Kucher, J.C. Bricker, M.E. Reno, R.S. Haizmann, Fuel Process. Technol. 35 (1993) 183.
[11] S. Kuba, M. Che, R.K. Grasselli, H. Knozinger, J. Phys. Chem. B 107 (2003) 3459.
[12] S.G. Ryu, B.C. Gates, Ind. Eng. Chem. Res. 37 (1998) 1786.
[13] N. Essayem, Y. Ben Taârit, C. Feche, P.Y. Gayraud, G. Sapaly, C. Naccache, J. Catal. 219 (2003) 97.
[14] J.K. Lee, H.K. Rhee, in: H.G. Karge, J. Weitkamp (Eds.), Zeolite Science 1994: Recent Progress and Discussions Studies in Surface Science and Catalysis, vol. 98, Elsevier, Amsterdam, 1995, p. 169.
[15] K. Fottinger, H. Vinek, Catal. Lett. 97 (2004) 131.
[16] A.P.E. York, P.H. Cuong, P.D. Gallo, M.J. Ledoux, Catal. Today 35 (1997) 51.
[17] K.I. Patrylak, F.M. Babonych, Yu.G. Voloshyna, M.M. Levchuk, V.G. Il'in, O.M. Yakovenko, I.A. Manza, I.M. Tsupryk, Appl. Catal. 174 (1998) 187.
[18] A. Chica, A. Corma, J. Catal. 187 (1999) 167.
[19] J.A. Moreno, G. Poncelet, Appl. Catal. 210 (2001) 151.
[20] S. Kuba, B.C. Gates, R.K. Grasselli, H. Knozinger, Chem. Commun. 321 (2001).
[21] R.M. Jao, T.B. Lin, J.R. Chang, J. Catal. 161 (1996) 222.
[22] D.G. Barton, S.L. Soled, E. Iglesia, Top. Catal. 6 (1998) 87.
[23] S. Kuba, P. Lukinskas, R.K. Grasselli, B.C. Gates, H. Knözinger, J. Catal. 216 (2003) 353.
[24] M. Guemini, Y. Rezgui, A. Tighezza, A. Bouchemma, Can. J. Chem. Eng. 82 (1) (2004) 184.
[25] Y. Rezgui, M. Guemini, Appl. Catal. 282 (2005) 45.
[26] S.-T. Wong, T. Li, S. Cheng, J.-F. Lee, C.-Y. Mou, Appl. Catal. 296 (2005) 90.
[27] P. Canizares, A. de Lucas, J.L. Valverde, F. Dorado, Ind. Eng. Chem. Res. 36 (1997) 4797.
[28] D.L. Hoang, H. Berndt, H. Miessener, E. Schereier, J. Volter, H. Lieske, Appl. Catal. 114 (1994) 295.
[29] B. Mile, M.A. Stirling, M.A. Zanmitt, J. Mol. Catal. 62 (1990) 179.
[30] M.D. Romero, J.A. Calles, A. Rodriguez, Ind. Eng. Chem. Res. 36 (1997) 3533.
[31] A. Scholz, B. Schnyder, A. Wokaun, J. Mol. Catal. 138 (1999) 249.
[32] C.U.I. Odebrand, A. Bahamonde, P. Avilar, J. Blanco, Appl. Catal. B 5 (1994) 117.
[33] J. Leyrer, R. Margraf, E. Taglauer, H. Knözinger, Surf. Sci. 201 (1988) 603.
[34] J. Kijenski, A. Baiker, M. Glinski, P. Dollenmeier, A. Wokaun, J. Catal. 101 (1986) 1.
[35] M. Schraml-Marth, A. Wokaun, A. Baiker, J. Catal. 124 (1990) 86.
[36] M. Campanati, G. Fornasari, A. Vaccari, Catal. Today 77 (2003) 299.
[37] M. Signoretto, M. Scarpa, F. Pinna, G. Strkul, P. Canton, A. benedetti, J. Non-Cryst Solids 225 (1998) 178.
[38] Y. Rezgui, M. Guemini, Appl. Catal. A: Gen. 355 (2008) 103.
[39] Y. Rezgui, M. Guemini, A. Tighezza, A. Bouchemma, Catal. Lett. 87 (1–2) (2003) 11.
[40] Y. Rezgui, M. Guemini, Energy Fuels 21 (2007) 602.
[41] G. Boskovic, R. Micic, P. Pavlovic, P. Putanov, Catal. Today 65 (2001) 123.
[42] T.N. Vu, J. van Gestel, J.P. Gilsona, C. Collet, J.P. Dathb, J.C. Duchet, J. Catal. 231 (2005) 468.
[43] M.D. Romero, J.A. Calles, A. Rodriguez, J.C. Cabanelas, Ind. Eng. Chem. Res. 37 (1998) 3846.
[44] M.D. Romero, A. de Lucas, J.A. Calles, A. Rodriguez, Appl. Catal. 146 (1996) 425.
[45] A. Lucas, P. Sanchez, F. Dorado, M.J. Ramos, J.L. Valverde, Appl. Catal. 294 (2005) 215.
[46] G. Larsen, L.M. Petkovic, Appl. Catal. 148 (1996) 155.
[47] A. Katrib, V. Logie, N. Saurel, P. Wehrer, L. Hilaire, G. Maire, Surf. Sci. 377–379 (1997) 754.
[48] A. Katrib, V. Logie, M. Peter, P. Wehrer, L. Hilaire, G. Maire, J. Chim. Phys. 94 (1997) 1923.
[49] S.R. Vaudagna, R.A. Comelli, N.S. Figoli, Appl. Catal. 164 (1997) 265.
[50] R.S. Drago, N. Kob, J. Phys. Chem. B 101 (1997) 3360.
[51] M.M. Telkar, J.M. Nadgeri, C.V. Rode, R.V. Chaudhari, Appl. Catal. 295 (2005) 23.
[52] M.G. Falco, S.A. Canavese, R.A. Comelli, N.S. Figoli, Appl. Catal. 201 (2000) 37.
[53] M. Hino, K. Arata, Appl. Catal. 169 (1998) 151.
[54] F. Alvarez, F.R. Ribeiro, G. Perot, C. Thomazeau, M. Guisnety, J. Catal. 162 (1996) 179.
[55] H.W. Kouwenhoven, Molecular sieves, ACS Advances in Chemistry Series, vol. 121, Am. Chem. Society, Washington, 1973, p. 529.
[56] M.H. Jordao, V. Simoes, D. Cardoso, Appl. Catal. 319 (2007) 1.
[57] A. Zhang, I. Nakamura, K. Aimuto, K. Fujimoto, Ind. Eng. Chem. Res. 34 (1995) 1074.
[58] J. Hu, K. Vernkaesh, J. Tierney, I. Wender, Appl. Catal. 114 (1994) 179.
[59] H. Liu, V. Adevva, G. Lei, W. Sachtler, J. Mol. Catal. 100 (1995) 35.
[60] J.C. Yori, C.R. Vera, J.M. Parera, Appl. Catal. 163 (1997) 165.
[61] J.M. Grau, J.C. Yori, J.M. Parera, Appl. Catal. 213 (2001) 247.
[62] D.G. Barton, S.L. Soled, G.D. Meitzner, G.A. Fuentes, E. Iglesia, J. Catal. 181 (1999) 57.
[63] S.V. Filimonova, A.V. Nosov, M. Scheithauer, H. Knözinger, J. Catal. 198 (2001) 89.
[64] E. Iglesia, D.G. Barton, S.L. Soled, S. Miseo, J.E. Baumgartner, W.E. Gates, G.A. Fuentes, G.D. Meitzner, Stud. Surf. Sci. Catal. 101 (1996) 533.
[65] S. Kuba, P. Lukinskas, R. Ahmad, F.C. Jentoft, R.K. Grasselli, B.C. Gates, H. Knözinger, J. Catal. 219 (2003) 376.
[66] C. Bigey, L. Hilaire, G. Maire, J. Catal. 198 (2001) 208.
[67] C. Bigey, L. Hilaire, G. Maire, J. Catal. 184 (1999) 406.
[68] W. Hua, J. Sommer, Appl. Catal. 232 (2002) 129.
[69] R. Roldan, F.J. Romero, C.J. Sanchidrian, J.M. Marinas, J.P. Gomez, Appl. Catal. 288 (2005) 104.
[70] T.D. Pope, J.F. Kriz, M. Stanciulescu, J. Monnier, Appl. Catal. 233 (2002) 45.